Title

Hand-held high-resolution fluorescence imaging system for fluorescence-guided surgery of patient and cell-line pancreatic tumors growing orthotopically in nude mice

Journal

Journal of Surgical Research, 187(2)

ISSN

0022-4804

Authors

Hiroshima, Yukihiko
Maawy, Ali
Sato, Sho
et al.

Publication Date

2014-04-01

DOI

10.1016/j.jss.2013.11.1083

Peer reviewed

Published in final edited form as:
J Surg Res. 2014 April ; 187(2): 510–517. doi:10.1016/j.jss.2013.11.1083.

Hand-Held High-Resolution Fluorescence Imaging System for Fluorescence-Guided Surgery of Patient and Cell-Line Pancreatic Tumors Growing Orthotopically in Nude Mice

Yukihiko Hiroshima[1,2,3], **Ali Maawy**[2], **Sho Sato**[3], **Takashi Murakami**[3], **Fuminari Uehara**[1,2], **Shinji Miwa**[1,2], **Shuya Yano**[1,2], **Masashi Momiyama**[3], **Takashi Chishima**[3], **Kuniya Tanaka**[3], **Michael Bouvet**[2], **Itaru Endo**[3], and **Robert M. Hoffman**[1,2]

[1] AntiCancer, Inc., San Diego, CA

[2] Department of Surgery, University of California San Diego, San Diego, CA

[3] Department of Gastroenterological Surgery, Yokohama City University Graduate School of Medicine, Yokohama, Japan

Abstract

Background—In this study, we investigated the advantages for fluorescence-guided surgery (FGS) in mice of a portable hand-sized imaging system compared to a large chamber fluorescing imaging system or a long-working-distance fluorescence microscope.

Methods—Mouse models of human pancreatic cancer for FGS included (1) MiaPaCa-2-expressing green fluorescent protein (GFP), (2) BxPC3 labeled with anti-CEA antibody conjugated with Alexa 488, (3) patient-derived orhotopic xenograft (PDOX)™ labeled with anti-CA19-9 antibody conjugated with Alexa 488.

Results—Each device could clearly detect the primary MiaPaCa-2-GFP. tumor and any residual tumor after FGS. In the BxPC3 model labeled with Alexa 488-conjugated anti-CEA, each device could detect the primary tumor, but the MVX10 could not clearly detect the residual tumor remaining after FGS while the other devices could. In the PDOX™ model labeled with Alexa 488 conjugated with anti CA19-9, only the portable hand-held device could distinguish the residual tumor from the background, and complete resection of the residual tumor was achieved under fluorescence navigation.

Conclusions—The results described in the present report suggest the hand-held mobile imaging system can be able to be applied to the clinic for FGS due to its convenient size and high sensitivity and help make FGS widely-used.

Keywords

Fluorescent proteins; pancreatic cancer; CEA; CA19-9; human patient tumor PDOXTM; cell line; mouse model; in vivo imaging; fluorescence-guided surgery

Correspondence to: Michael Bouvet, MD, Department of Surgery, University of California San Diego, Moores Cancer Center, 3855 Health Sciences Drive #0987, La Jolla, CA 92093-0987, mbouvet@ucsd.edu.

1 Introduction

The complete detection of tumors at the time of surgery is vital in optimizing surgical resection. The means to make tumors glow offers great advantages for tumor detection enabling fluorescence-guided surgery (FGS) and a number of different approaches have been attempted to label and image tumors during surgery (1-8).

We have previously demonstrated the enhanced visualization and detection of primary and metastatic lesions with the use of telomerase-dependent adenovirus (OBP-401) that expresses the *gfp* gene only in cancer cells for use in fluorescence-guided surgery (FGS) (9-11). We have also demonstrated the use of fluorescent-labeled antibodies (12-17) administered to the tumor-bearing mice for successful FGS of metastatic cancer in mouse models.

However, the FGS studies described above have used large complex imaging systems, such as the OV100 (Olympus Corporation, Tokyo, Japan) and the MVX10 Macro View (Olympus Corporation, Center Valley, Pennsylvania), which would not be useful in the clinic. What is currently needed for clinical application of FGS is a simpler and more convenient imaging system to be used in the operating room (OR).

In the present study, we compared a hand-held completely mobile fluorescence imaging system to the conventional *in vivo* imaging systems for the detection of pancreatic cancer in mouse models labeled with fluorescent proteins or fluorescent antibodies for effectiveness of FGS.

2 Materials and Methods

2.1 Establishment of green fluorescent protein labeled cancer cell line

The MiaPaCa-2 human pancreatic cell line was stably transfected with green fluorescent protein (GFP) as previously described (18-20). In brief, cells were incubated with a 1:1 precipitated mixture of retroviral supernatants of PT67-GFP cells and RPMI 1640 (Irvine Scientific, Santa Ana, CA) containing 10 % fetal bovine serum (FBS) (Hyclone Laboratories, Logan, UT) for 72 h. Fresh medium was replenished at this time. Cells were harvested with trypsin/EDTA 72 h post-transduction and subcultured at a ratio of 1:15 into selective medium, which contained 200 μg/ml of G418. The level of G418 was increased stepwise up to 800 μg/ml (18-22).

2.2 Cell culture

MiaPaCa-2-GFP and BxPC3 human pancreatic cancer cells were maintained in RPMI 1640 medium supplemented with 10% fetal bovine serum (FBS). The cells were incubated at 37 °C in a humidified atmosphere of 5% CO_2 in air. The cells were collected after trypsinization and stained with trypan blue (Sigma-Aldrich, St. Louis, MO). Only viable cells were counted with a hemocytometer (Hausser Scientific, Horsham, PA).

2.3 Animals

Athymic NCR nude mice (*nu/nu*) (AntiCancer, Inc., San Diego, CA) at 4-6 weeks of age were used in this study. Mice were kept in a barrier facility under HEPA filtration. Mice were fed with autoclaved laboratory rodent diet. All surgical procedures and imaging were performed with the animals anesthetized by intramuscular injection of 0.02 ml of a solution of 50% ketamine, 38% xylazine, and 12% acepromazine maleate. All animal studies were conducted in accordance with the principals and procedures outlined in the NIH Guide for the Care and Use of Laboratory Animals under PHS Assurance Number A3873-1.

2.4 Subcutaneous tumor cell implantation

MiaPaCa-2-GFP and BxPC3 cells were harvested by trypsinization and washed twice with serum-free medium. Cells (2×10^6 in 100 μl serum-free media) were injected subcutaneously, within 30 min of harvesting, over the right and left flanks in male nu/nu mice between 4 and 6 weeks of age. Subcutaneous tumors were allowed to grow for 2-4 weeks until large enough to supply adequate tumor to harvest for subsequent orthotopic implantation (23).

2.5 Establishment of patient derived orthotopic xenograft (PDOX™) of pancreatic cancer

Pancreatic cancer patient tumor tissue was obtained at surgery and cut into 3-mm^3 fragments and transplanted subcutaneously in NOD/SCID mice (24-26). The patient tumors were then harvested from the NOD/SCID mice and passed orthotopically in nude mice (21-24, 27). All patients provided informed consent and the study was conducted under the approval of the Institutional Review Board of the UC San Diego Medical Center.

2.6 Orthotopic tumor implantation

A small 6- to 10-mm transverse incision was made on the left flank of the mouse through the skin and peritoneum. The tail of the pancreas was exposed through this incision and a single 3-mm^3 tumor fragment from subcutaneous tumors was sutured to the tail of the pancreas using 8-0 nylon surgical sutures (Ethilon; Ethicon Inc., NJ, USA). On completion, the tail of the pancreas was returned to the abdomen, and the incision was closed in one layer using 6-0 nylon surgical sutures (Ethilon) (21-24, 27).

2.7 Antibody conjugation

Monoclonal antibodies specific for carcinoembryonic antigen (CEA) or carbohydrate antigen 19-9 (CA19-9) were purchased from RayBiotech, Inc. (Norcross, GA) or Abcam, Inc (Cambridge, MA). The antibodies were labeled with the AlexaFluor 488 Protein Labeling Kit (Molecular Probes Inc., Eugene, OR) according to the manufacturer's instructions and as previously described (12).

2.8 Fluorescence imagings

The Dino-Lite digital camera (AM4113T-GFBW Dino-Lite Premier; AnMo Electronics Corporation, Taiwan) [Fig. 1], the Olympus OV100 Small Animal Imaging System (Olympus Corp.), containing an MT-20 light source (Olympus Biosystems, Planegg, Germany) and DP70 CCD camera (Olympus Corp., Tokyo, Japan), (28) and the MVX10 Macro View (Olympus Corp.) with FluoCam 1500G color CCD camera were used for imaging fluorescent tumors in live mice (29). Whole-body images were taken by the OV100 with a magnification of 0.14×. High magnification images were taken by the OV100 with a magnification of 0.56× or 0.89×. The Dino-Lite has a magnification range of 30× to 50×. The MVX10 has a magnification range of 0.63× to 3.2×.

2.9 Mobile high-resolution fluorescence imaging system

The portable Dino-Lite mobile imaging system was used for imaging in live mice [Fig. 1A]. The portable system has 7 filtered (wavelength) blue LEDs for excitation lighting and with an 510 nm emission filter and 1 white LED switched by software, and a 1.3 megapixel sensor. This digital camera can magnify from 30× up to 200× and can readily take both pictures and videos of magnified green fluorescent objects. The camera's dimensions are 10.5 cm × 3.2 cm and the weight is only 105 g [Fig. 1C]. This all-in-one compact digital camera makes the Dino-Lite imaging system easily transportable [Fig. 1B].

2.10 Tumor resection

Four to eight weeks after orthotopic implantation, surgery was performed on tumor-bearing mice. A monoclonal anti-CEA or anti-CA19-9 antibody conjugated with Alexa 488 was delivered to the mice with the BxPC3 tumor or the pancreatic cancer PDOX™, respectively, as a single intravenous dose 24 hours before surgery. A midline incision was made in the abdomen of tumor-bearing mice, and the exposed pancreatic tumor was imaged preoperatively with the OV100, the Dino-Lite and the MVX10 under both standard bright-field and fluorescence illumination. Resection of the primary pancreatic tumor was performed under standard bright-field. Postoperatively, the surgical resection bed was imaged with the OV100, the Dino-Lite and the MVX10 under both standard bright-field and fluorescence illumination to assess the completeness of surgical resection. Resection of the residual tumor of PDOX™ was performed using the Dino-Lite under fluorescence navigation.

3 Results and Discussion

3.1 Imaging pancreatic cancer in mouse models

We imaged three tapes of pancreatic tumors in mouse models which were fluorescently labeled by different methods. A monoclonal anti-CEA or anti-CA19-9 antibody conjugated with Alexa 488 was delivered to the mice with the BxPC3 pancreatic tumor or pancreatic cancer PDOX™, respectively, as a single intravenous dose 24 hours before imaging. We have previously demonstrated that the fluorescence signal of a fluorophore-conjugated antibody was detectable at 30 min and reached its peak at 24 h after systemic antibody delivery in orthotopic human pancreatic tumor mouse models (13).

Tumors were imaged with the OV100, the Dino-Lite and the MVX10 before and after BLS. The MiaPaCa-2-GFP pancreatic tumor had the strongest fluorescence of the three tumors, and each device could clearly detect the primary tumor [Fig. 2A-C] and the residual tumor [Fig. 2D-G] after bright-light surgery (BLS). In the BxPC3 pancreatic tumor model, each device could also detect the primary tumor [Fig. 3A-C]. However the OV100 at a magnification of 0.14× (whole body) and the MVX10 at a magnification of 1.6× could not detect the residual tumor clearly because the fluorescence signal of the BxPC3 pancreatic tumor labeled with the antibody was not as strong as the signal of the genetically labeled MiaPaCa-2-GFP tumor [Fig. 3D and G]. In contrast, the residual tumor of the BxPC3 was visualized with the OV100 at a magnification of 0.56× [Fig. 3E] and the Dino-Lite at a magnification of 30× [Fig. 3F].

The pancreatic cancer PDOX™ labeled with the fluorescent anti CA19-9 antibody was more difficult to detect than the BxPC3 tumor labeled with the fluorescent anti-CEA antibody [Fig. 3 and 4]. The OV100, at a magnification of 0.14×, detected the PDOX™ primary tumor only at the same intensity as the autofluorescence of small intestine and stomach [Fig. 4A]. The MVX10, at a magnification of 1.6×, barely detected the signal of the tumor [Fig. 4D]. The OV100 at a magnification of 0.56× [Fig. 4B] and the Dino-Lite at a magnification of 30× [Fig. 4C] could distinguish the primary tumor from background, but the margin of the tumor was not clearly visualized with the OV100 but was clearly visualized with the Dino-Lite [Fig. 4B].

3.2 Complete resection of the residual PDOX™ tumor under fluorescence navigation with the portable imaging system

We have previously showed that FGS for pancreatic cancer decreased the residual tumor burden and improved overall and disease-free survival in mouse models (12-14). The fluorescence of the PDOX™ was too weak to distinguish the tumor from the background

with the conventional imaging devices OV100 and MVX10 [Fig. 4D and G]. However, the Dino-Lite mobile imaging system could clearly visualize not only the primary tumor [Fig. 4C] but also the residual tumor after BLS [Fig. 4F] in the PDOX™ model. Furthermore, we achieved the complete resection of the residual tumor under fluorescence navigation. This result suggests that the Dino-Lite mobile imaging system can be able to be applied to the clinic.

The ability to visualize primary tumor as well as small satellite tumors near the surgical margin that virtually go undetected under standard bright light surgery has had a significant impact in surgical outcomes in mouse models (9-15, 17). We have previously demonstrated that failure to remove these small deposits under BLS resulted in recurrence in a matter of months (14, 15, 17). Providing a more objective method of detecting tumor intraoperatively for better delineation of tumor from normal surrounding tissue can permit a more precise excision (1-8).

In the present study, the hand-held imaging system was compared to the larger previously-used imaging system for FGS for both relatively dimly-labeled tumors (BxPC-3 and the patient-derived xenograft and the brightly-labeled MiaPaCa-2 tumor). The hand-held device proved to be superior for all tumors. Future experiments will quantify the sensitivity of the hand-held imaging device compared to larger imaging systems.

4. Conclusions

The Dino-Lite mobile imaging fluorescence system is a hand-held and highly sensitive imaging system with advantages in sensitivity over much larger fluorescence imaging systems previously used for FGS. We achieved the complete resection of the residual tumor in the PDOX™ model using the mobile imaging system, suggesting this system can be able to be applied to the clinic in the near future to enable widespread application of FGS.

Acknowledgments

This study was supported in part by National Cancer Institute grant CA126023 and 142669 and Grants-in-Aid from the Japanese Ministry of Education, Culture, Sports, Science and Technology for Fundamental Research(C) (#23592018 to I.E and # 24592009 to K.T).

References

1. Bouvet M, Hoffman RM. Glowing tumors make for better detection and resection. Sci Transl Med. 2011; 3:110fs110.
2. Nguyen QT, Olson ES, Aguilera TA, Jiang T, Scadeng M, Ellies LG, Tsien RY. Surgery with molecular fluorescence imaging using activatable cell-penetrating peptides decreases residual cancer and improves survival. Proc Natl Acad Sci U S A. 2010; 107:4317–4322. [PubMed: 20160097]
3. Stiles BM, Adusumilli PS, Bhargava A, Stanziale SF, Kim TH, Chan MK, Huq R, Wong R, Rusch VW, Fong Y. Minimally invasive localization of oncolytic herpes simplex viral therapy of metastatic pleural cancer. Cancer Gene Ther. 2006; 13:53–64. [PubMed: 16037824]
4. Stummer W, Pichlmeier U, Meinel T, Wiestler OD, Zanella F, Reulen HJ. Fluorescence-guided surgery with 5-aminolevulinic acid for resection of malignant glioma: a randomised controlled multicentre phase III trial. Lancet Oncol. 2006; 7:392–401. [PubMed: 16648043]
5. Tran Cao HS, Kaushal S, Menen RS, Metildi CA, Lee C, Snyder CS, Talamini MA, Hoffman RM, Bouvet M. Submillimeter-resolution fluorescence laparoscopy of pancreatic cancer in a carcinomatosis mouse model visualizes metastases not seen with standard laparoscopy. J Laparoendosc Adv Surg Tech A. 2011; 21:485–489. [PubMed: 21699431]

6. Troyan SL, Kianzad V, Gibbs-Strauss SL, Gioux S, Matsui A, Oketokoun R, Ngo L, Khamene A, Azar F, Frangioni JV. The FLARE intraoperative near-infrared fluorescence imaging system: a first-in-human clinical trial in breast cancer sentinel lymph node mapping. Ann Surg Oncol. 2009; 16:2943–2952. [PubMed: 19582506]
7. Urano Y, Sakabe M, Kosaka N, Ogawa M, Mitsunaga M, Asanuma D, Kamiya M, Young MR, Nagano T, Choyke PL, Kobayashi H. Rapid cancer detection by topically spraying a gamma-glutamyltranspeptidase-activated fluorescent probe. Sci Transl Med. 2011; 3:110ra119.
8. van Dam GM, Themelis G, Crane LM, Harlaar NJ, Pleijhuis RG, Kelder W, Sarantopoulos A, de Jong JS, Arts HJ, van der Zee AG, Bart J, Low PS, Ntziachristos V. Intraoperative tumor-specific fluorescence imaging in ovarian cancer by folate receptor-alpha targeting: first in-human results. Nat Med. 2011; 17:1315–1319. [PubMed: 21926976]
9. Kishimoto H, Aki R, Urata Y, Bouvet M, Momiyama M, Tanaka N, Fujiwara T, Hoffman RM. Tumor-selective, adenoviral-mediated GFP genetic labeling of human cancer in the live mouse reports future recurrence after resection. Cell Cycle. 2011; 10:2737–2741. [PubMed: 21785265]
10. Kishimoto H, Kojima T, Watanabe Y, Kagawa S, Fujiwara T, Uno F, Teraishi F, Kyo S, Mizuguchi H, Hashimoto Y, Urata Y, Tanaka N. In vivo imaging of lymph node metastasis with telomerase-specific replication-selective adenovirus. Nat Med. 2006; 12:1213–1219. [PubMed: 17013385]
11. Kishimoto H, Zhao M, Hayashi K, Urata Y, Tanaka N, Fujiwara T, Penman S, Hoffman RM. In vivo internal tumor illumination by telomerase-dependent adenoviral GFP for precise surgical navigation. Proc Natl Acad Sci U S A. 2009; 106:14514–14517. [PubMed: 19706537]
12. Kaushal S, McElroy MK, Luiken GA, Talamini MA, Moossa AR, Hoffman RM, Bouvet M. Fluorophore-conjugated anti-CEA antibody for the intraoperative imaging of pancreatic and colorectal cancer. J Gastrointest Surg. 2008; 12:1938–1950. [PubMed: 18665430]
13. McElroy M, Kaushal S, Luiken GA, Talamini MA, Moossa AR, Hoffman RM, Bouvet M. Imaging of primary and metastatic pancreatic cancer using a fluorophore conjugated anti-CA19-9 antibody for surgical navigation. World J Surg. 2008; 32:1057–1066. [PubMed: 18264829]
14. Metildi CA, Kaushal S, Hardamon CR, Snyder CS, Pu M, Messer KS, Talamini MA, Hoffman RM, Bouvet M. Fluorescence-guided surgery allows for more complete resection of pancreatic cancer, resulting in longer disease-free survival compared with standard surgery in orthotopic mouse models. J Am Coll Surg. 2012; 215:126–135. discussion 135-126. [PubMed: 22632917]
15. Metildi CA, Kaushal S, Lee C, Hardamon CR, Snyder CS, Luiken GA, Talamini MA, Hoffman RM, Bouvet M. An LED light source and novel fluorophore combinations improve fluorescence laparoscopic detection of metastatic pancreatic cancer in orthotopic mouse models. J Am Coll Surg. 2012; 214:997–1007. e1002. [PubMed: 22542065]
16. Tran Cao HS, Kaushal S, Metildi CA, Menen RS, Lee C, Snyder CS, Messer K, Pu M, Luiken GA, Talamini MA, Hoffman RM, Bouvet M. Tumor-specific fluorescence antibody imaging enables accurate staging laparoscopy in an orthotopic model of pancreatic cancer. Hepatogastroenterology. 2012; 59:1994–1999. [PubMed: 22369743]
17. Metildi CA, Kaushal S, Snyder CS, Hoffman RM, Bouvet M. Fluorescence-guided surgery of human colon cancer increases complete resection resulting in cures in an orthotopic nude mouse model. J Surg Res. 2013; 179:87–93. [PubMed: 23079571]
18. Hoffman RM, Yang M. Subcellular imaging in the live mouse. Nat Protoc. 2006; 1:775–782. [PubMed: 17406307]
19. Hoffman RM, Yang M. Color-coded fluorescence imaging of tumor-host interactions. Nat Protoc. 2006; 1:928–935. [PubMed: 17406326]
20. Hoffman RM, Yang M. Whole-body imaging with fluorescent proteins. Nat Protoc. 2006; 1:1429–1438. [PubMed: 17406431]
21. Katz MH, Takimoto S, Spivack D, Moossa AR, Hoffman RM, Bouvet M. A novel red fluorescent protein orthotopic pancreatic cancer model for the preclinical evaluation of chemotherapeutics. J Surg Res. 2003; 113:151–160. [PubMed: 12943825]
22. Tran Cao HS, Bouvet M, Kaushal S, Keleman A, Romney E, Kim G, Fruehauf J, Imagawa DK, Hoffman RM, Katz MH. Metronomic gemcitabine in combination with sunitinib inhibits multisite

metastasis and increases survival in an orthotopic model of pancreatic cancer. Mol Cancer Ther. 2010; 9:2068–2078. [PubMed: 20606044]

23. Hoffman RM. Orthotopic metastatic mouse models for anticancer drug discovery and evaluation: a bridge to the clinic. Invest New Drugs. 1999; 17:343–359. [PubMed: 10759402]
24. Furukawa T, Kubota T, Watanabe M, Kuo TH, Kase S, Saikawa Y, Tanino H, Teramoto T, Ishibiki K, Kitajima M, et al. Immunochemotherapy prevents human colon cancer metastasis after orthotopic onplantation of histologically-intact tumor tissue in nude mice. Anticancer Res. 1993; 13:287–291. [PubMed: 8517641]
25. Kim MP, Evans DB, Wang H, Abbruzzese JL, Fleming JB, Gallick GE. Generation of orthotopic and heterotopic human pancreatic cancer xenografts in immunodeficient mice. Nat Protoc. 2009; 4:1670–1680. [PubMed: 19876027]
26. Kim MP, Truty MJ, Choi W, Kang Y, Chopin-Lally X, Gallick GE, Wang H, McConkey DJ, Hwang R, Logsdon C, Abbruzzesse J, Fleming JB. Molecular profiling of direct xenograft tumors established from human pancreatic adenocarcinoma after neoadjuvant therapy. Ann Surg Oncol. 2012; 19(Suppl 3):S395–403. [PubMed: 21701930]
27. Fu X, Guadagni F, Hoffman RM. A metastatic nude-mouse model of human pancreatic cancer constructed orthotopically with histologically intact patient specimens. Proc Natl Acad Sci U S A. 1992; 89:5645–5649. [PubMed: 1608975]
28. Yamauchi K, Yang M, Jiang P, Xu M, Yamamoto N, Tsuchiya H, Tomita K, Moossa AR, Bouvet M, Hoffman RM. Development of real-time subcellular dynamic multicolor imaging of cancer-cell trafficking in live mice with a variable-magnification whole-mouse imaging system. Cancer Res. 2006; 66:4208–4214. [PubMed: 16618743]
29. Kimura H, Momiyama M, Tomita K, Tsuchiya H, Hoffman RM. Long-working-distance fluorescence microscope with high-numerical-aperture objectives for variable-magnification imaging in live mice from macro- to subcellular. J Biomed Opt. 2010; 15:066029. [PubMed: 21198203]

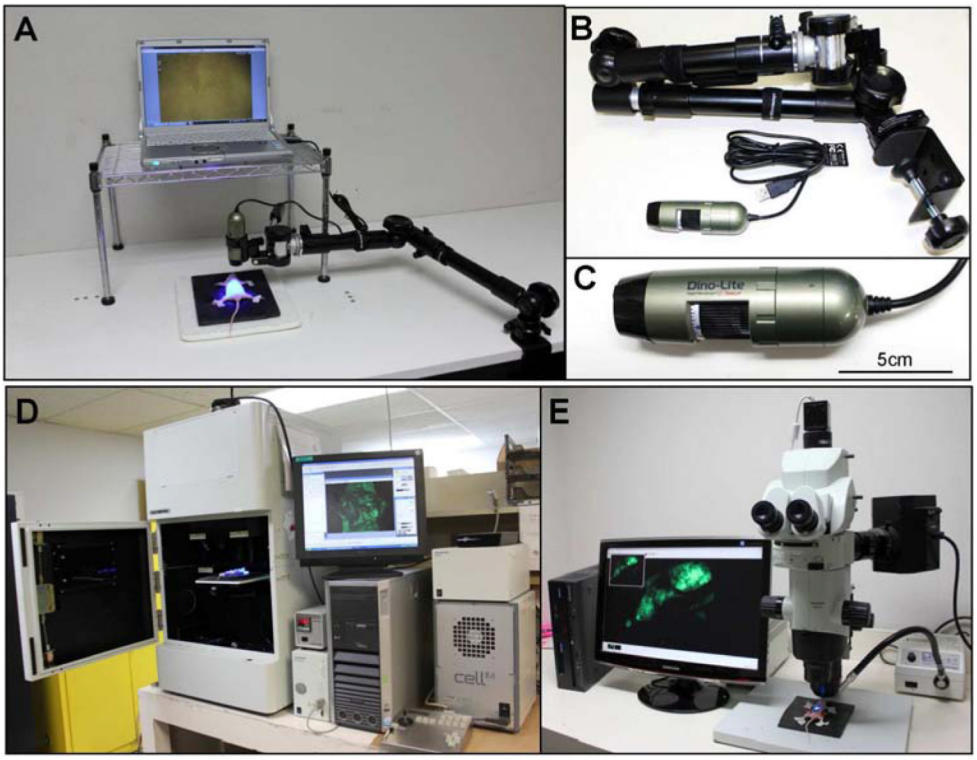

Fig. 1.

(A) Overview of the Dino-Lite mobile imaging system with a Dino-Lite digital camera. (B) The Dino-Lite mobile imaging system. (C) Close-up view of a Dino-Lite digital camera. The camera's dimensions are 10.5 cm × 3.2 cm and the weight is only 105 g. (D) Overview of the Olympus OV100 Small Animal Imaging System (Olympus Corp.). (E) Overview of the Olympus MVX10 Macro View (Olympus Corp.).

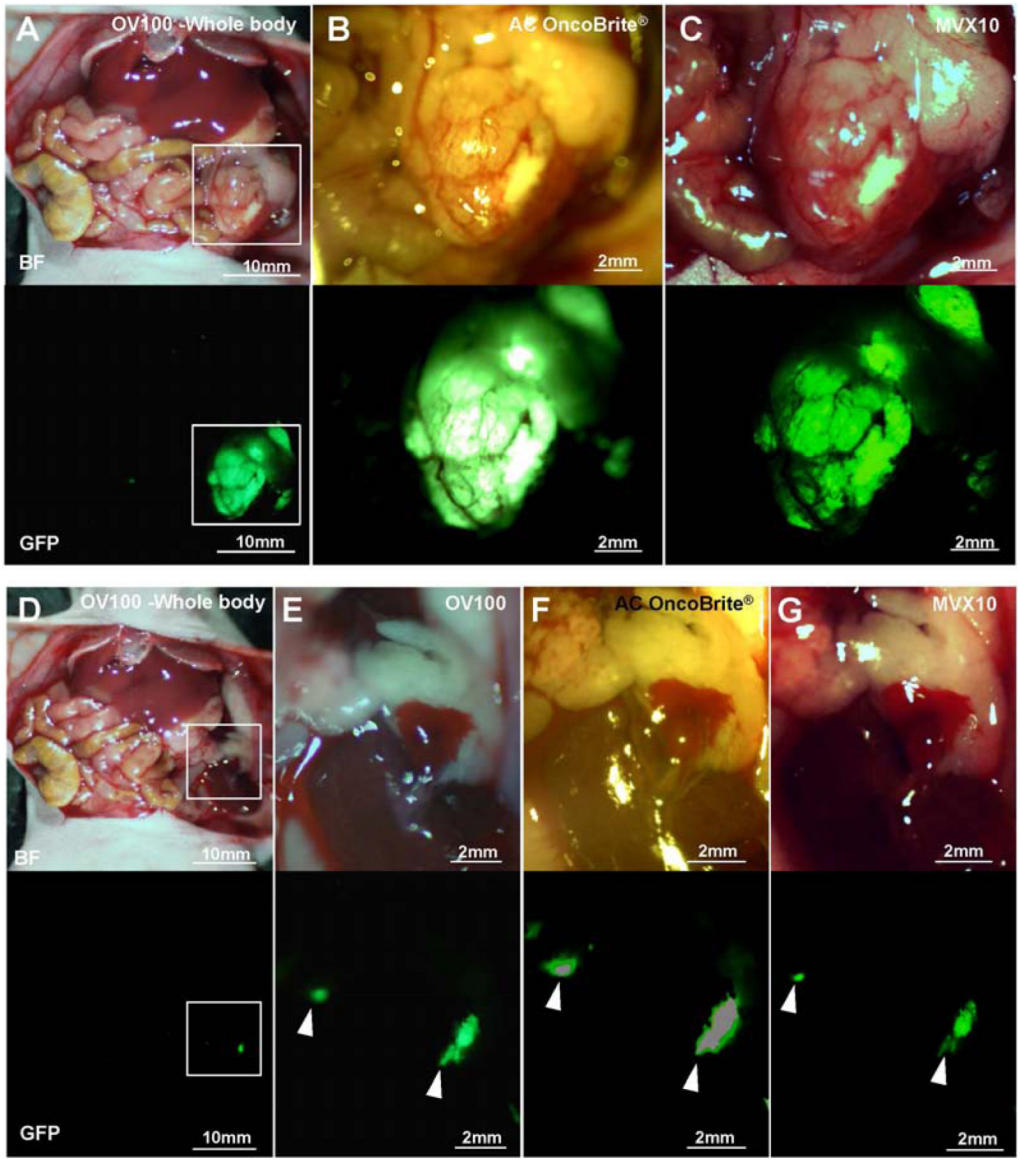

Fig. 2.

Imaging of genetically labeled MiaPaCa-2-GFP tumor. The primary MiaPaCa-2-GFP tumor was imaged with the OV100 at a magnification of 0.14× (A), the Dino-Lite at a magnification of 30× (B) and the MVX10 at a magnification of 1.6× (C). The residual tumor after BLS was imaged with the OV100 at a magnification of 0.14× and 0.56× (D and E, respectively), the Dino-Lite at a magnification of 30× (F), and the MVX10 at a magnification of 1.6× (G). Boxes in (A) indicate the view areas of (B) and (C), and boxes in (D) indicate the view areas of (E), (F) and (G). White arrow heads indicate the detected residual tumors after BLS.

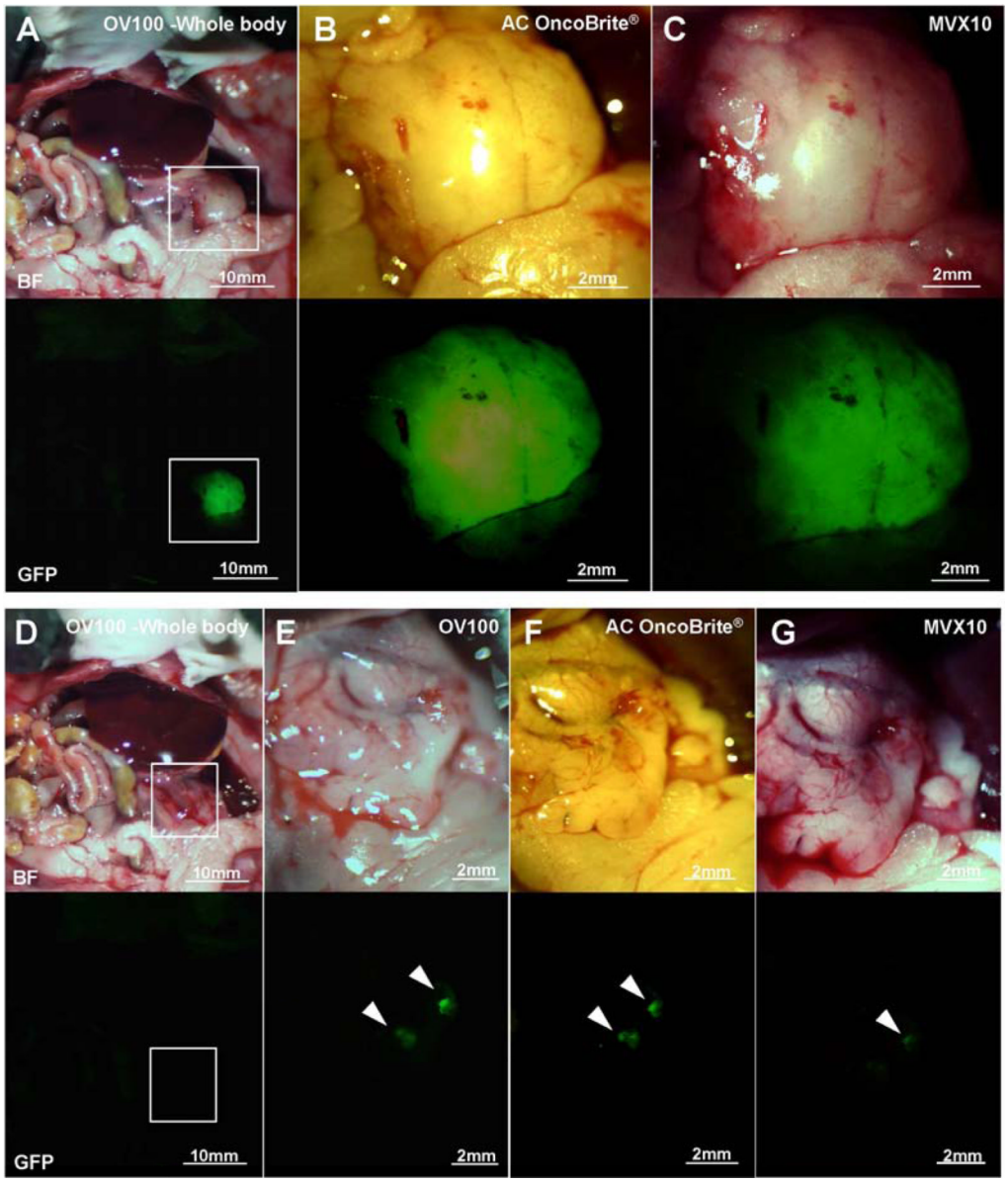

Fig. 3.

Imaging of BxPC3 tumor labeled with fluorescent anti-CEA antibody. The primary BxPC3 tumor labeled with fluorescent anti-CEA antibody was imaged with the OV100 at a magnification of 0.14× (A), the Dino-Lite at a magnification of 30× (B) and the MVX10 at a magnification of 1.6× (C). The residual tumor after BLS was imaged with the OV100 at a magnification of 0.14× and 0.56× (D and E), the Dino-Lite at a magnification of 30× (F) and the MVX10 at a magnification of 1.6× (G). Boxes in (A) indicate the view areas of (B) and (C), and boxes in (D) indicate the view areas of (E), (F) and (G). White arrow heads indicate the detected residual tumors after BLS.

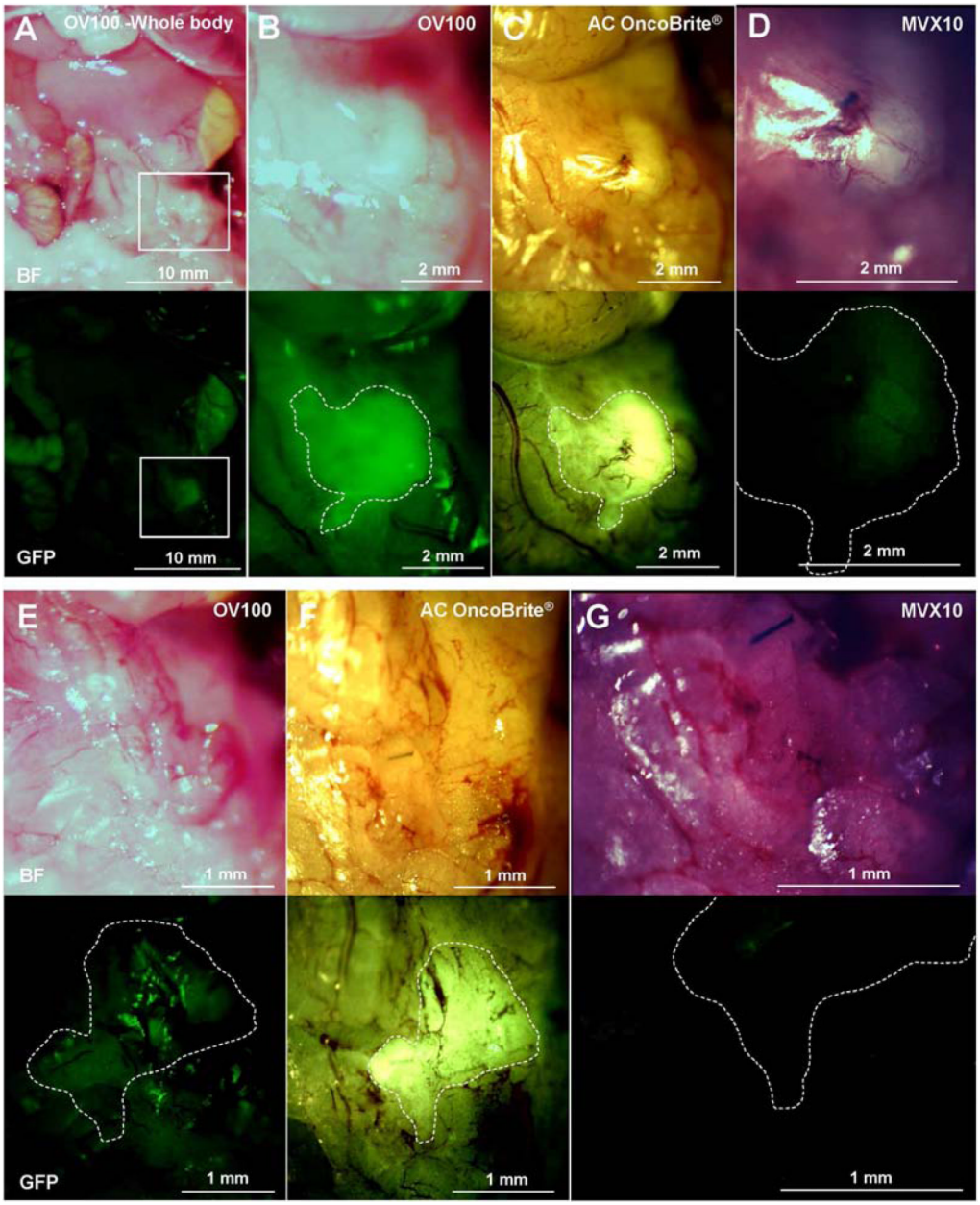

Fig. 4.

Imaging of PDOX tumor labeled with fluorescent anti-CA19-9 antibody. The primary PDOX tumor, labeled with fluorescent anti-CA19-9 antibody, was imaged with the OV100 at a magnification of 0.14× and 0.56× (A and B), the Dino-Lite at a magnification of 30× (C) and the MVX10 at a magnification of 1.6× (D). The MVX10 at a magnification of 3.2× did not detect any signals from the residual tumor (G). The OV100 at a magnification of 0.89× could not distinguish the residual tumor from background (E). The Dino-Lite at a magnification of 50× could clearly distinguish the residual tumor from background (F). Boxes in (A) indicate the view areas of (B), (C) and (D). The areas surrounded by white broken lines indicate the estimated residual tumor areas after BLS.